Proc. Natl. Acad. Sci. USA
Vol. 91, pp. 316–320, January 1994
Biochemistry

Cysteine-rich LIM domains of LIM-homeodomain and LIM-only proteins contain zinc but not iron

(LIM domains/Isl-1/zinc fingers/RBTN)

V. E. V. ARCHER*, J. BRETON†, I. SANCHEZ-GARCIA*, H. OSADA*, A. FORSTER*, A. J. THOMSON†, AND T. H. RABBITTS*

*Medical Research Council Laboratory of Molecular Biology, Hills Road, Cambridge CB2 2QH, United Kingdom; and †University of East Anglia, School of Chemical Sciences, Norwich NR4 7TJ, United Kingdom

Communicated by Aaron Klug, September 21, 1993 (received for review July 20, 1993)

ABSTRACT **The structure of LIM domains has major implications for transcription because proteins such as Isl-1 contain two LIM domains associated with a homeodomain, and RBTN1/Ttg-1 and RBTN2/Ttg-2 contain two LIM domains but no homeodomain. Conserved cysteine and histidine residues in the LIM domains suggest a metal-binding role. RBTN and Isl-1 LIM proteins have been made in *Escherichia coli* and insect cell expression systems and their metal content has been determined using atomic absorption spectroscopy and electron paramagnetic resonance spectroscopy. LIM proteins expressed in soluble form contain zinc atoms, whereas bacterial inclusion bodies invariably also have Fe–S clusters. The latter are identified as linear $[Fe_3S_4]^+$ clusters and appear to result from incorrect metal coordination by *E. coli*. These studies show that RBTN1, RBTN2, and Isl-1 are metalloproteins that contain zinc but not iron and, therefore, that the LIM domain represents a zinc-binding domain.**

The LIM domain is a cysteine-rich motif found in proteins of many species. There are two known classes of LIM proteins; those that encode only LIM domains (LIM-only) and those with LIM domains plus other motifs such as homeodomains (LIM-homeodomain). The latter contains two LIM domains and include the original group of LIM proteins (*Lin*-11, *Isl*-1, *Mec*-3) (1–3). LIM proteins lacking homeodomains are equally diverse and include proteins with one, two, or three LIM domains. This group includes the dual LIM-domain proteins RBTN1/Ttg-1 (4–6) and RBTN2/Ttg-2 (7, 8) that are involved in childhood T-cell acute leukemias.

The arrangement of conserved cysteine and histidine residues within the LIM motif, $CX_2CX_{17\text{-}19}HX_2CX_2CX_2CX_{16\text{-}20}CX_2D/H/C$, resembles other metal-binding protein motifs. These include the zinc fingers of DNA binding proteins (1, 2, 6, 9) and the Fe–S clusters of the electron transport protein ferredoxin (1, 2, 7). Previous studies have found zinc in LIM proteins extracted from natural eukaryotic sources, such as the single-LIM-domain cysteine-rich intestinal protein (CRIP) (10), the double-LIM-domain cysteine-rich protein (cCRP), and the treble-LIM-domain protein zyxin (11), and also in bacterially produced cCRP (12). However, zinc and iron are both present in the LIM-homeodomain protein lin-11 expressed as inclusion bodies in *Escherichia coli* (13). We have studied the metal binding associated with the LIM-homeodomain protein Isl-1 and the LIM-only proteins RBTN1 and RBTN2 produced in bacterial and insect-cell expression systems. Our results show that all three proteins possess zinc atoms but give no evidence of native Fe–S centers. These data indicate that the LIM motif corresponds to a zinc-binding domain.

The publication costs of this article were defrayed in part by page charge payment. This article must therefore be hereby marked "*advertisement*" in accordance with 18 U.S.C. §1734 solely to indicate this fact.

MATERIALS AND METHODS

Expression Plasmids. The *E. coli* vectors pGEX-3X (14) and pMALc (New England Biolabs) were used to prepare pGEX-RBTN1, pGEX-RBTN2, pMALc-RBTN1, pMALc-RBTN2, and pMALc-Isl-1. pGEX-KG (15) was used for construction of pGEX-Isl-1 and pGEX-CMYC. The pGEX-Isl-1 clone and all pMALc clones contain full-length LIM proteins. pGEX-RBTN2 and pGEX-RBTN1 contain RBTN proteins lacking only the first one or two amino acids, respectively. The CMYC insert of pGEX-CMYC extends from codon 347 to the C-terminal end (16). The Tramtrack (*ttk*) zinc-finger expression clone D911zf was cloned into pET11 and contains two zinc fingers, corresponding to aa 499–561 (17). pT7ERDBD was an 84-aa peptide of the estrogen receptor cloned into the T7 expression system (18).

Preparation of Bacterial Fusion Proteins. Bacterial inclusion bodies were prepared as described (19). The final pellets were suspended in 10 mM Tris·HCl, pH 7.5/0.1 mM EDTA, packed into electron paramagnetic resonance (EPR) tubes, and frozen in liquid nitrogen. For whole-cell EPR, induced cells were washed with ice-cold phosphate-buffered saline (PBS), ice-cold PBS containing 10 mM EDTA (pH 7.5), and ice-cold 0.8% NaCl, before preparing a slurry in 0.8% NaCl for EPR spectroscopy.

Soluble MBP fusion proteins (where MBP is the *E. coli malE* gene product) were prepared as follows: exponential cultures of bacteria were induced at 37°C for 3–4 h with 0.3 mM isopropyl β-D-thiogalactoside. Bacteria were resuspended in 0.05 culture volume of amylose resin column buffer [20 mM Hepes, pH 7.9/150 mM NaCl/1–10 mM dithiothreitol/1 mM NaN_3/pepstatin A (1 μg/ml)/aprotinin (1 μg/ml)/leupeptin (1 μg/ml)/1 mM phenylmethylsulfonyl fluoride] and frozen at −20°C. Thawed bacteria were ruptured by four 30-s sonication bursts or by passage twice through a French pressure cell. The lysate was cleared (10,000 × *g* for 30 min at 4°C), diluted 1:5 with column buffer, filtered, and applied to amylose resin (New England Biolabs). Fusion protein was eluted with column buffer containing 10 mM maltose. Column fractions were analyzed by SDS/PAGE on 10% gels. Samples were prepared with Ar-gassed solutions and stored under Ar.

For anaerobic bacterial lysates for EPR spectroscopy, cells were grown and induced as above, washed with 1 mM EDTA, and frozen at −20°C under argon. Pellets were thawed in a nitrogen atmosphere glove box, suspended in 400 μl of 50 mM Tris·HCl, pH 8.0/25% (wt/vol) sucrose/50 μM ZnOAc/10 mM dithiothreitol/lysozyme (0.8 mg/ml), and incubated for 30 min. $MgCl_2$ and DNase I were added to 10 mM and 10 μg/ml, respectively, and incubated for 30 min. Lysate was centrifuged

Abbreviations: cCRP, cysteine-rich protein; EPR, electron paramagnetic resonance; MCD, magnetic circular dichroism; AAS, atomic absorption spectroscopy; GST, glutathione *S*-transferase.

at 10,000 × *g* for 10 min at 4°C and the supernatant was packed into EPR tubes and frozen in liquid nitrogen.

Production of RBTN1 Protein in Insect Cells. Murine RBTN1 was cloned into the baculovirus transfer vector pVL1393. Sf9 (*Spodoptera frugiperda* ovary) cells were maintained as described (20). Sf9 cells were transfected using the BaculoGold transfection kit (Pharmingen). Recombinant virus was plaque-purified and used to infect 10^7 Sf9 cells for 4 days at 27°C. Virus concentration was amplified by two further passages of Sf9 cell infection. For EPR analysis, 1.2 × 10^8 Sf9 cells were infected with 1.2 × 10^9 plaque-forming units of wild-type *Autographa californica* multiple nuclear polyhedrosis virus or passage 3 recombinant RBTN virus in 20 ml of TNM-FH (20) for 2 h at room temperature. Cells were diluted into 100 ml of fresh TNM-FH and incubated for a further 48 h at 27°C. Cells were washed with 1 mM EDTA in PBS and made into a thick paste that was loaded into EPR tubes and frozen in liquid nitrogen.

EPR and Magnetic Circular Dichroism (MCD) Spectroscopy. Low-temperature EPR spectra were recorded with a Bruker ER200D X-band spectrometer, equipped with an ESR-900 continuous flow cryostat (Oxford) and a DTC-2 temperature controller (Oxford). Dithionite reduction was performed by incubating the samples for 10–30 min with excess sodium dithionite in an anaerobic glove box. MCD spectra (21) were recorded using a JASCO-J500D spectropolarimeter. The magnetic field was generated by a split-coil superconducting magnet, Spectromag-4 (Oxford). To measure spectra of insoluble inclusion bodies, a thin film of RBTN paste was smeared between two quartz plates. The assembly was loaded into a SM4 cryostat.

Atomic Absorption Spectroscopy (AAS). AAS of MBP fusions was carried out with a Perkin Elmer 3100 impact bead spectrometer (with Zn and Fe standards). Protein samples were prepared and purified using solutions prepared with Analar grade reagents and MilliQ metal-free water.

RESULTS AND DISCUSSION

LIM and Zinc-Finger Proteins Contain Iron When in Bacterial Inclusion Bodies. The LIM-homeodomain protein Isl-1

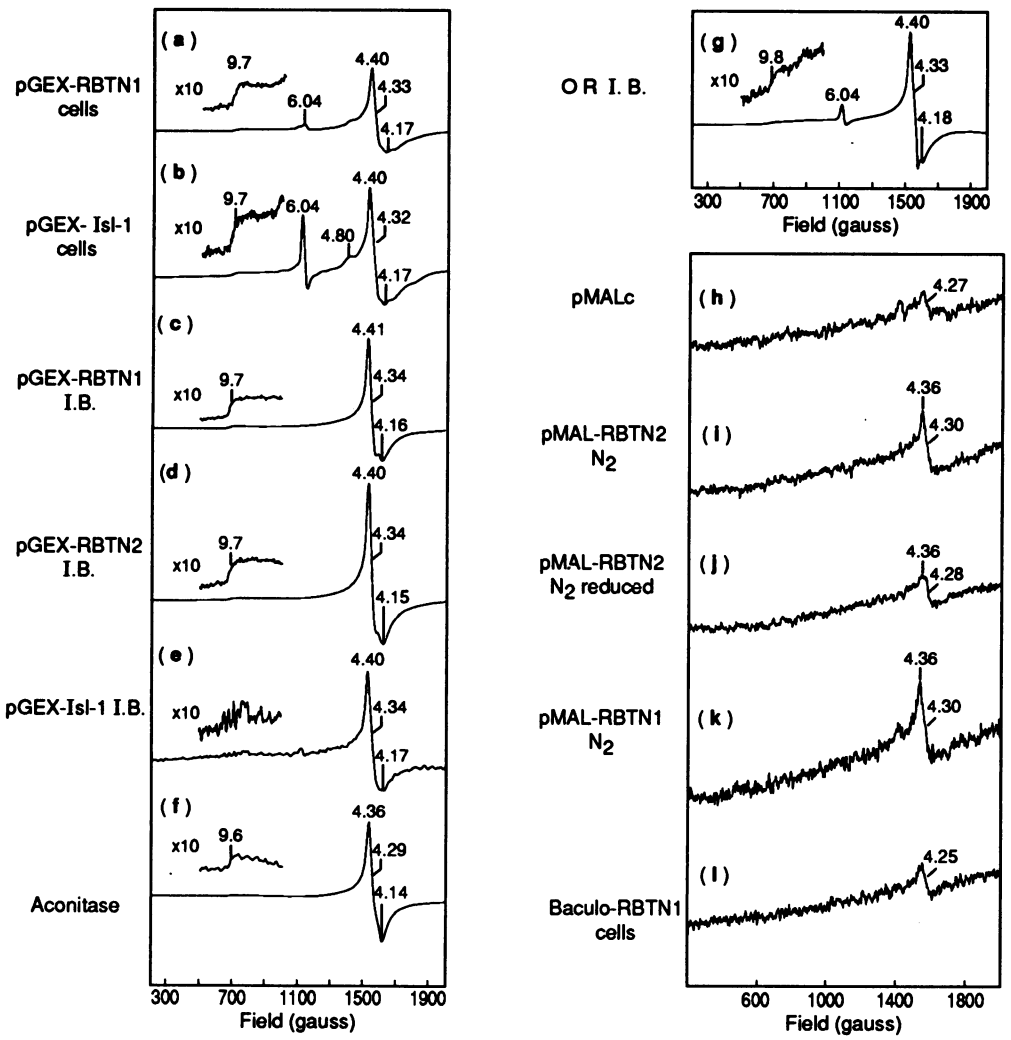

FIG. 1. X-band EPR spectroscopy of proteins from bacterial and insect cells expressing LIM and zinc-finger proteins. Spectra were obtained with a microwave frequency of 9.40 GHz, a power of 2 mW, and a modulation amplitude of 10 G (1 G = 0.1 mT). The numbers on the figures are *g* values calculated from the magnetic fields and indicate only the positions of features of the spectra (i.e., they are not necessarily true *g* values). Spectra: a, GST–RBTN1 whole cells, a gain of 5 × 10^4, a temperature of 10 K; b, GST–Isl-1 whole cells, a gain of 2 × 10^5, a temperature of 10 K; c, GST–RBTN1 inclusion bodies, a gain of 2.5 × 10^4, a temperature of 11.5 K; d, GST–RBTN2 inclusion bodies, a gain of 6.3 × 10^4, a temperature of 10 K; e, GST–Isl-1 inclusion bodies, a gain of 1 × 10^5, a temperature of 4.5 K; f, purple aconitase solution in 50 mM Hepes, pH 7.5/50% (vol/vol) ethanediol, a gain of 1 × 10^5, a temperature of 10 K; g, estrogen receptor inclusion bodies, a gain of 1.25 × 10^5, a temperature of 4.5 K; h, MBP only, a gain of 8 × 10^5, a temperature of 9 K; i, MBP–RBTN2 prepared under N_2, a gain of 5 × 10^5, a temperature of 10 K; j, MBP–RBTN2 prepared under N_2 followed by dithionite reduction, a gain of 8 × 10^5, a temperature of 10 K; k, MBP–RBTN1 prepared under N_2, a gain of 8 × 10^5, a temperature of 10 K; l, RBTN1-expressing Sf9 cells, a gain of 8 × 10^5, a temperature of 10 K.

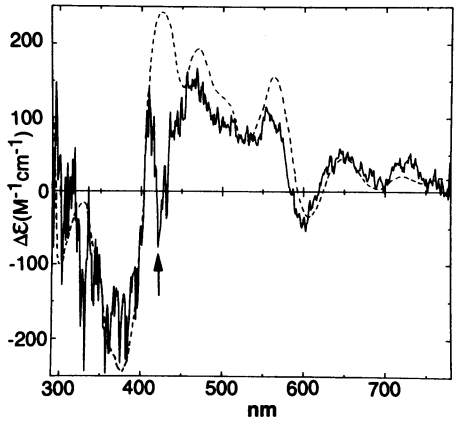

FIG. 2. MCD spectroscopy of RBTN2 inclusion body protein compared to purple aconitase. Low-temperature MCD spectra of purple aconitase (dashed line) and RBTN2 inclusion bodies (solid line). The conditions were, for aconitase, 50 mM Hepes, pH 7.5/50% ethanediol and a temperature of 1.6 K and, for RBTN2, 10 mM Tris·HCl, pH 7.7/0.1 mM EDTA/50% (vol/vol) glycerol, a temperature of 4.2 K, and a magnetic field of 5 T. The arrow indicates a feature due to heme impurity in the RBTN2 sample.

(2) and the LIM-only proteins RBTN1 (5–7) and RBTN2 (7, 8) were prepared as recombinant fusion proteins, in *E. coli* cells, using either the pGEX vector system, which employs fusion with the glutathione *S*-transferase (GST) protein, or the pMALc vector system, which employs fusion with the *E. coli malE* gene product (MBP). Isl-1 was also produced in bacteria using a T7 promoter expression system and eukaryotic RBTN1 was also produced in insect cells. Analysis of the clones used in this study was carried out by DNA sequencing to ensure fidelity of PCR amplification and protein quality was assessed by SDS/PAGE and Western blot analysis.

Preliminary examination showed that GST–RBTN fusion proteins were associated with brown-colored insoluble inclusion bodies (data not shown). Only ≈10% of the GST–Isl-1 and 30% of the T7-produced Isl-1 proteins were soluble. Since the insoluble GST fusion proteins were brown,

Table 1. Metal content of soluble LIM proteins determined by AAS

Construct	Atoms, no. per molecule of protein	
	Zn	Fe
pGEX-Isl-1	4.0	0.3
	7.8	0.7
	1.9	0.12
T7-Isl	0.76	0.35
	1.83	0.59
pMALc-Isl-1	2.61	0.44
	4.34	0.52
pMALc-RBTN1	1.84	0.27
	1.43	0.26
	5.63	0.39
	9.66	0.39
	7.01	0.19
pMALc-RBTN2	1.70	0.52
	1.65	0.64
	3.64	0.68
	2.30	0.59
	5.67	0.43
	4.19	0.44
Estrogen receptor	0.9	ND

Each entry represents metal determination of separate preparations of the protein indicated. ND, none detectable.

indicating the presence of iron, we carried out EPR spectroscopy using whole bacterial cells in which most of the protein was recombinant protein. The EPR spectra of cells containing RBTN1 and Isl-1 (Fig. 1, spectra a and b) display several resonances, notably in the $g = 6$ and $g = 2$ regions. However, only the broad asymmetric peak around $g = 4.3$ is unique to the transformed cells. The $g = 6.04$ resonance probably arises from high-spin ferric heme species, and the signals at $g = 4.3$ are undoubtedly contributed by both mononuclear high-spin Fe(III) and Fe–S-containing proteins, since these signals are not observed in untransformed *E. coli* cells.

The purity of the RBTN1, RBTN2, and Isl-1 samples was increased by preparation of inclusion bodies. All three proteins gave similar EPR spectra with $g = 4.3$ peaks as the main resonance (Fig. 1, spectra c–e, respectively). Further inspection of the spectra of the LIM inclusion bodies reveals a low-field resonanance at $g = 9.7$ with a step shape. The intensity of this signal decreased rapidly with increased sample temperature, whereas the $g = 4.3$ signal was still present at temperatures up to 50 K. Inclusion bodies containing a GST–CMYC fusion protein, which has no LIM domain, were also prepared for EPR spectroscopy. A signal at $g = 4.3$ is observed but is weaker and much narrower than the RBTN or Isl-1 signals and is characteristic of adventitiously bound high-spin Fe(III) ions (data not shown).

Hence, the LIM proteins give rise to EPR signals at $g = 4.3$ and 9.7 arising from a species containing Fe(III). Two known structures would fit this EPR spectrum, namely, a monomeric tetrathiolato-Fe(III) analogous to that in the electron transfer protein rubredoxin (21) or a linear Fe–S cluster core $[Fe_3S_4]^+$ coordinated by four thiolate groups such as in the so-called "purple" aconitase (22, 23), an inactive form of the protein formed at high pH. The EPR spectrum of purple aconitase (Fig. 1, spectrum f) is remarkably similar to the signal obtained from the LIM proteins. This similarity with purple aconitase was further established by MCD spectroscopy of a sample of RBTN2 inclusion body protein (Fig. 2). Despite a rather poor signal-to-noise ratio caused by the scattering nature of the sample and the low concentration of iron, the similarity between the two is clear. The MCD spectrum of rubredoxin in the oxidized state is quite different in form and intensity (21). Thus, both EPR and MCD spectroscopy indicate a linear $[Fe_3S_4]^+$ cluster is present in the inclusion bodies of RBTN1, RBTN2, and Isl-1. Reduction of samples with dithionite failed to elicit any new signals; therefore, the presence of the more widespread $[Fe_4S_4]^{2+}$ cluster core is unlikely. Nevertheless, the $[Fe_4S_4]^{2+}$ cluster can be resistant to reduction in some proteins (24).

Since the linear $[Fe_3S_4]^+$ cluster is unknown in any native protein, the presence of this cluster in LIM proteins is probably a consequence of expression of the protein in a bacterial host. Two eukaryotic zinc-finger proteins, the estrogen receptor (C_4 class) (18) and Ttk (C_2H_2 class) (17), were synthesized in *E. coli* as inclusion bodies and examined by EPR spectroscopy. In both cases, a broad $g = 4.3$ signal was observed (Fig. 1, spectrum g, shows the results for the estrogen receptor). The signals appear to be an overlap of a sharp derivative at $g = 4.3$ due to adventitious mononuclear Fe(III) and of the broader signal due to the linear $[Fe_3S_4]^+$ cluster. The presence of the latter is confirmed by the signal at $g = 9.7$–9.8. Thus, the expression of cysteine-rich proteins in *E. coli* as inclusion bodies can lead to the artificial incorporation of Fe–S clusters.

LIM Proteins Contain Zinc but not Iron in Their Soluble Form. The metal content of LIM proteins expressed in soluble form was investigated to obviate artefacts of this type. A scan for all metals in the Isl-1, RBTN1, and RBTN2 proteins revealed only zinc and iron, and AAS results for these metals are summarized in Table 1. Analysis of the

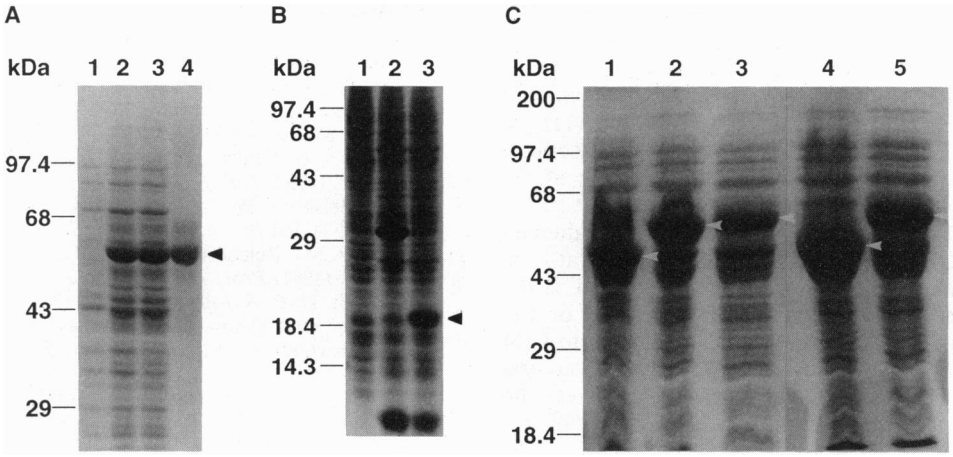

FIG. 3. SDS/PAGE of purified soluble LIM proteins and cell extracts used for EPR analysis. SDS/PAGE of protein samples used in AAS and EPR spectroscopic analyses. Molecular mass markers shown are myosin (200 kDa), phosphorylase (97.4 kDa), bovine serum albumin (68 kDa), ovalbumin (43 kDa), carbonic anhydrase (29 kDa), β-lactoglobulin (18.4 kDa), and lysozyme (14.3 kDa). (*A*) Aerobically prepared protein from pMALc-RBTN2 transformed DH5α. Lanes: 1, uninduced cells; 2, total cell lysate from isopropyl β-D-thiogalactoside-induced cells; 3, total soluble protein from induced cells; 4, amylose-resin-purified MBP–RBTN2. (*B*) Sf9 whole-cell extracts. Lanes: 1, uninfected cells; 2, wild-type *Autographa californica* multiple nuclear polyhedrosis virus (AcMNPV)-infected cells; 3, AcMNPV-RBTN1-infected cells. (*C*) Anaerobically (N_2) and aerobically (O_2) prepared soluble bacterial extracts. Lanes: 1, MBP (N_2); 2, MBP–RBTN1 (N_2); 3, MBP–RBTN2 (N_2); 4, MBP (O_2); 5, MBP–RBTN2 (O_2).

soluble fraction of GST–Isl-1 showed variation in zinc content but averaged ≈3.4 Zn atoms per molecule (Table 1). MBP–Isl-1 protein contained an average of 2.6 Zn atoms per molecule. This compares with a determined value of 0.9 Zn atom per molecule of a two-zinc-finger estrogen receptor protein. In all preparations of soluble Isl-1, ≈0.5 Fe atom was found per molecule of protein (Table 1). The cysteine and histidine residues per LIM domain could accommodate up to 2 Zn atoms or a maximum of 4 Zn atoms per Isl-1 molecule. On the other hand, the Fe–S centers of the $[Fe_3S_4]^+$ type would require 3 or 6 Fe atoms per LIM domain. The relative molar quantities of iron and zinc, therefore, suggest that zinc, not iron, is structurally present in LIM domains. These conclusions were supported by EPR analysis of the soluble Isl-1 preparations, which showed only weak signals with *g* values consistent with a linear $[Fe_3S_4]^+$ center (data not shown). These results suggest that the $[Fe_3S_4]^+$ centers are present in non-native minority forms of the protein.

Unlike the GST–RBTN proteins, which were essentially insoluble, MBP–RBTN fusions yielded significant amounts of soluble fusion protein, which was prepared on amylose resin columns and compared to the total soluble protein fraction from induced cells by SDS/PAGE (Fig. 3*A*). EPR results obtained with purified MBP–RBTN proteins (139 μM) showed no significant signals (data not shown). These purified fractions were also analyzed by AAS (Table 1). The average zinc content was 3–5 Zn atoms per molecule of protein; the maximum iron content was 0.64 Fe atom per molecule of protein. EPR spectroscopy of these samples also yielded only very weak signals, indicating insignificant iron content.

To investigate the effect of oxygen on potential Fe–S clusters, soluble MBP–RBTN fusion protein extracts were prepared both anaerobically and aerobically. MBP–RBTN fusion proteins prepared in this way were assayed by SDS/PAGE to estimate the fusion protein molarity of the solutions (Fig. 3*C*). Roughly equal amounts of protein were present in cell extracts prepared under O_2 or N_2 and the molarities were estimated to be between 90 and 160 μM. MBP–RBTN2 samples (N_2) were subjected to EPR analysis (Fig. 1, spectrum i) and after reduction with sodium dithionite (Fig. 1, spectrum j). The spectra reveal only a weak signal at $g = 4.3$ (compared to MBP only in Fig. 1, spectrum h) and gave no evidence for the presence of the linear $[Fe_3S_4]^+$ cluster. Similarly, MBP–RBTN1 protein, prepared under identical conditions, failed to reveal any significant EPR signals. Only weak signals were observed at high gain (Fig. 1, spectrum k) and these probably emanate from a small amount of contaminating insoluble protein fraction.

Thus the RBTN1/2 soluble fusion proteins do not seem to have physiologically relevant Fe–S centers. However since ferredoxin proteins expressed in soluble form in *E. coli* sometimes fail to incorporate clusters (25), RBTN1 protein has been expressed in insect cells using the baculovirus system. SDS/PAGE analysis of cells expressing RBTN1 compared to wild-type-virus-infected cells (Fig. 3*B*) indicated an approximate molarity of 200 μM for the RBTN1 protein. Whole Sf9 cells, infected with the RBTN1 virus, were frozen directly in liquid nitrogen and analyzed by EPR at high gain. No signal was detected, which indicates the absence of Fe–S centers (Fig. 1, spectrum 1). Thus neither the soluble bacterial nor the eukaryotic LIM proteins contain detectable Fe–S clusters.

LIM Is a Zinc-Binding Domain. In the absence of a biological assay to establish correct metal content and coordination, we have relied on different expression systems to insert metal into the LIM domain. Our data show that the LIM proteins Isl-1, RBTN1, and RBTN2, when produced in soluble form, have only zinc as a coordinated metal. This is consistent with previous work on zyxin (11, 26) and CRP (10–12). The demonstration of a Fe–S core cluster, linear $[Fe_3S_4]^+$, in the LIM domain is probably not relevant since we have found this cluster in the zinc-finger proteins Ttk and estrogen receptor. Data from the insect host cell expression gives strong support to the proposal that the LIM domains do not contain iron and represent a zinc binding motif.

Unlike GATA (27), our data render unlikely the possibility of an *in vivo* Fe coordination in the LIM domain. Substitution of metals is not uncommon such as the replacement, in cCRP, of Zn(II) by Co(II) in a pseudotetrahedral metal coordination site (12). However, the steric requirements for the binding of an iron in a tetrahedral array of four ligands requires a cavity for metal coordination that is larger than for zinc. Therefore, we would not expect to see substitution of zinc or iron without a change in protein conformation.

A number of functions are possible for LIM domains. The existence of LIM-only proteins such as RBTN1 and RBTN2 is suggestive of a domain important in DNA–protein or protein–protein interactions (28). Zyxin is a LIM protein that binds to α-actinin and to the LIM protein cCRP (11). In addition, the LIM domains of Isl-1 have an inhibitory effect, thought to be intramolecular, on the DNA binding of the associated homeodomain (29). Homology between the LIM domain and the DNA-binding GATA-like "finger" domain suggests that the LIM domain, like GATA (27), has at least partly a DNA binding function (I.S.G., H.O., and T.H.R., unpublished observations). The recent structure of the GATA-1 DNA binding domain may have relevance to LIM domain structure and function (30). Complete structural analyses of LIM domains will be necessary to reveal the nature of the zinc interaction and allow the function of this domain to be elucidated.

V.E.V.A., J.B., and I.S.-G. have made equal contributions to this work. We thank Dr. J. E. Dixon for providing the pGEX-KG vector, L. Fairall and D. Rhodes for the clone D9113F, J. Schwabe and D. Rhodes for the clone pT7ERDBD, S. Medd for advice on preparation of inclusion bodies, and K. Johnson for advice on pGEX. We thank Mr. A. P. Dickerson for the atomic absorption analyses. V.E.V.A. was supported by the Human Frontier Science Programme. H.O. and I.S.-G. were supported by the Leukaemia Research Fund. The work at the University of East Anglia was supported by the Science and Engineering Research Council.

1. Freyd, G., Kim, S. K. & Horvitz, H. R. (1990) *Nature (London)* **344,** 876–879.
2. Karlsson, O., Thor, S., Norberg, T., Ohlsson, H. & Edlund, T. (1990) *Nature (London)* **344,** 879–882.
3. Way, J. C. & Chalfie, M. (1988) *Cell* **54,** 5–16.
4. Boehm, T., Baer, R., Lavenir, I., Forster, A., Waters, J. J., Nacheva, E. & Rabbitts, T. H. (1988) *EMBO J.* **7,** 385–394.
5. Boehm, T., Greenberg, J. M., Buluwela, L., Lavenir, I., Forster, A. & Rabbitts, T. H. (1990) *EMBO J.* **9,** 857–868.
6. McGuire, E. A., Hockett, R. D., Pollock, K. M., Bartholdi, M. F., O'Brien, S. J. & Korsmeyer, S. J. (1989) *Mol. Cell. Biol.* **9,** 2124–2132.
7. Boehm, T., Foroni, L., Kaneko, Y., Perutz, M. P. & Rabbitts, T. H. (1991) *Proc. Natl. Acad. Sci. USA* **88,** 4367–4371.
8. Royer-Pokora, B., Loos, U. & Ludwig, W.-D. (1991) *Oncogene* **6,** 1887–1893.
9. Liebhaber, S. A., Emery, J. G., Urbanek, M., Wang, X. & Cooke, N. E. (1990) *Nucleic Acids Res.* **18,** 3871–3879.
10. Hempe, J. M. & Cousins, R. J. (1991) *Proc. Natl. Acad. Sci. USA* **88,** 9671–9674.
11. Sadler, I., Crawford, A. W., Michelsen, J. W. & Beckerle, M. C. (1992) *J. Cell Biol.* **119,** 1573–1587.
12. Michelsen, J. W., Scheichel, K. L., Beckerle, M. C. & Winge, D. R. (1993) *Proc. Natl. Acad. Sci. USA* **90,** 4404–4408.
13. Li, P. M., Reichert, J., Freyd, G., Horvitz, H. R. & Walsh, C. T. (1991) *Proc. Natl. Acad. Sci. USA* **88,** 9210–9213.
14. Smith, D. B. & Johnson, K. S. (1988) *Gene* **67,** 31–40.
15. Guan, K. & Dixon, J. E. (1991) *Anal. Biochem.* **192,** 262–267.
16. Blackwood, E. M. & Eisenman, R. N. (1991) *Science* **251,** 1211–1217.
17. Harrison, S. D. & Travers, A. A. (1990) *EMBO J.* **9,** 207–216.
18. Schwabe, J. W. R., Neuhaus, D. & Rhodes, D. (1990) *Nature (London)* **348,** 458–461.
19. Nagai, K. & Thogersen, H. C. (1987) *Methods Enzymol.* **153,** 461–481.
20. Summers, M. D. & Smith, G. E. (1987) *A Manual of Methods for Baculovirus Vectors and Insect Cell Culture Procedures* (Tex. Agric. Exp. Stn., College Station, TX).
21. Thomson, A. J., Cheesman, M. R. & George, S. J. (1993) *Methods Enzymol.* **226,** 199–232.
22. Kennedy, M. C., Kent, T. A., Emptage, M. H., Merkle, H., Beinert, H. & Munck, E. (1984) *J. Biol. Chem.* **259,** 14463–14471.
23. Richards, A. J. M., Thomson, A. J., Holm, R. H. & Hagen, K. S. (1990) *Spectrochim. Acta* **46A,** 987–993.
24. Thomson, A. J. (1993) *Curr. Biol.* **3,** 173–174.
25. Bourdineaud, J. P., Howard, S. P., Pages, J. M., Bernadac, A., Leroy, G., Bruschi, M. & Lazdunski, C. (1990) *Biochimie* **72,** 407–415.
26. Crawford, A., Michelsen, J. W. & Beckerle, M. C. (1992) *J. Cell Biol.* **116,** 1381–1393.
27. Omichinski, J. G., Trainor, C., Evans, T., Gronenborn, A. M., Clore, G. M. & Felsenfeld, G. (1993) *Proc. Natl. Acad. Sci. USA* **90,** 1676–1680.
28. Rabbitts, T. H. & Boehm, T. (1990) *Nature (London)* **346,** 418.
29. Sanchez-Garcia, I., Osada, H., Forster, A. & Rabbitts, T. H. (1993) *EMBO J.* **12,** 4243–4250.
30. Omichinski, J. G., Clore, G. M., Schaad, O., Felsenfeld, G., Trainor, C., Appella, E., Stahl, S. J. & Gronenborn, A. M. (1993) *Science* **261,** 438–446.